Available online at www.sciencedirect.com

ScienceDirect

International Journal of Mass Spectrometry 265 (2007) 1–14

International Journal of Mass Spectrometry

www.elsevier.com/locate/ijms

Electron-impact ionization of benzoic acid, nicotinic acid and their *n*-butyl esters: An approach to regioselective proton affinities derived from ionization and appearance energy data

Joachim Opitz

Institut für Organische Chemie, Universität Stuttgart, Pfaffenwaldring 55, D-70569 Stuttgart, Deutschland, Germany

Received 4 December 2006; received in revised form 17 April 2007; accepted 23 April 2007

Abstract

Electron-impact ionization mass spectra, the decay of metastable ions, ionization and appearance energies and bond energies, as dissociation energies, are reported for the title compounds. An ionization energy of 9.47 eV was obtained for benzoic acid, 9.43 eV for benzoic acid *n*-butyl ester, 9.61 eV for nicotinic acid and 9.97 eV for nicotinic acid *n*-butyl ester.

Molecular ions of both butyl esters show two common main fragmentation pathways: the first process is a McLafferty rearrangement, characterized by the transfer of one H-atom from the aliphatic ester chain, which leads to the ions of either the organic acid or 1-butene. From their appearance energies and known thermodynamic data, gas-phase formation enthalpies (ΔH_f^0) of the parent *n*-butyl esters are calculated. Values of $\Delta H_f^0 = (-4.29 \pm 0.3)$ eV for benzoic acid *n*-butyl ester and $\Delta H_f^0 = (-3.66 \pm 0.3)$ eV for nicotinic acid *n*-butyl ester were obtained.

The second process is characterized by the transfer of two H-atoms from the ester chain leading to a protonated form of the corresponding organic acids and C_4H_7 radicals. Good evidence is provided for the formation of methylallyl radicals. Appearance energies are used to calculate a proton affinity (PA) for benzoic acid. The obtained value of $PA = (8.73 \pm 0.3)$ eV, corresponding to a protonation of the carbonyl group, is in close corroboration with published data ($PA = 8.51$ eV). Activation energies for the intermediate H-transfers were found to be insignificant. This methodic gateway is applied to the system of nicotinic acid and its butyl ester. Adopting the formation of a methylallyl radical, the obtained proton affinity of nicotinic acid, $PA = 8.58$ eV, is very near to the published data of benzoic acid. An alternative fragmentation mechanism leading to a value of $PA \approx 9.5$ eV (typical for a protonation of the pyridine-nitrogen) is very unlikely. It is concluded that this transfer of two H-atoms from the ester chain is controlled by a charge switching between the carboxylic oxygen atoms which leads to a regiospecific protonation site, in this case to the protonated carbonyl group. This is conform with a B3LYP DFT calculation with a corresponding proton affinity of $PA = 8.29$ eV.

Keywords: Single or double H-transfer; CO_2 elimination; Activation energy; Enthalpies formation; Cation affinity

1. Introduction

Mass spectrometric ionization and appearance energies (IE, AE) are a valuable tool for the evaluation of detailed ionic fragmentation mechanisms and, particularly, of thermodynamic properties of ions and of neutral molecules and fragments as well. Offering a wider application range, some of the accessible data can be compared with results of competing methods like photoelectron spectroscopy (PES) and combustion calorimetry.

While PES is a reliable source of ionization energies of molecules, the limitations of combustion calorimetry are difficulties in the product analysis, especially in the case of organometallic compounds. Well-known obstacles of mass spectrometric methods, leading to experimentally higher minimum threshold energy values, are the formation of ions with internal excess energy in a vertical excitation or the kinetic shift [1,2], in cases where the formation of ions is too slow to allow a detection at the true energetic threshold conditions.

Moreover, for the evaluation of thermochemical data from appearance energies, the internal energies of the products have to be addressed. In the theoretic extreme, all internal energy of the educt is concentrated into the reactive coordinate and the products are left with an internal temperature of 0 K [3,4]. On the time scale of the decay of a polyatomic molecule, this needs an efficient vibrational coupling under collisionless conditions

---

E-mail address: joachim.opitz@oc.uni-stuttgart.de.

1387-3806/$ – see front matter © 2007 Elsevier B.V. All rights reserved.
doi:10.1016/j.ijms.2007.04.014

by far beyond the accidental resonant coupling case. However, at least for simple dissociation reactions on electron-impact ionization, good evidence is provided that, at most, only a small part of the initial internal energy of the educt contributes to the reaction energy in such an intramolecular collisionless fragmentation. Therefore, the products are regarded to be formed near to the original sample temperature [4]. This modified picture means that the reservoir of the excitation energy is efficiently coupled only with the corresponding reaction coordinate, which centers in the concept of excited local modes. Important for the evaluation of experimental data, however, most of the temperature dependence actually arises from the vibrational heat capacity and these changes are usually not exceeding the experimental error limit of the AE measurements (see Appendix A).

During our investigations of laser-induced multiphoton ionization/dissociation processes of organic [5–7] and organometallic [8–15] compounds, we found that carefully calibrated ionization and appearance energies obtained on electron-impact (EI) ionization can be compared very well with the absorbed photon energies for the formation of a specific ion. Organometallic compounds which decompose to their bare metal ions allow the determination of their formation enthalpies based on the well-known ionization energies and enthalpies of formation of these metal ions. Thermochemical investigations of organic compounds, however, are sometimes sophisticated due to their tendency to extensive H-shifts, migration of entire functional groups and, not at least, the lack of necessary reliable thermodynamic data.

Small organic molecules, however, appear to be challenging targets. Therefore, this method has recently been extended to suited organic compounds, where reliable formation enthalpies of intermediate fragment ions are accessible from protonated smaller neutral molecules using their known enthalpies of formation and their proton affinities. Mandelic acid and mandelic acid methyl ester, as prototypes for the $C_6H_5CH(OH)$–X system [15] and triphenylmethanol, as a prototype for the $(C_6H_5)_2C(OH)$–X system [16], were studied.

For many molecules, the ionic fragmentation process results in fragments actually representing the protonated form of a well-known stable neutral molecule.

In reverse, appropriate reliable ionization and appearance energy data are a gateway to the direct determination of proton affinities of these neutrals.

A promising target into such investigations are organic carboxyl esters, where the ionic fragmentation strongly depends on the length of the aliphatic ester chain.

Beginning with the ethyl esters, the (classical) McLafferty rearrangement with the transfer of a γ-H-atom from the ester chain to the carbonyl oxygen results in the formation of ions of the pure organic acid. It has been shown that the origin of the itinerant H-atom in this rearrangement is highly specific. For benzoic acid propyl ester, deuterium labelling of the propyl group showed, that, on EI ionization at 70 eV, C-2-propyl-hydrogens were transferred with a probability of 86%, becoming higher at lower internal excess energy.

Beginning with propyl esters, a competitive mechanism, denoted as a double McLafferty rearrangement, becomes operative. This mechanism is characterized by the transfer of two H-atoms resulting in the formation of the protonated form of the organic acid. With a lesser specifity, double H-transfer involved one H-atom from the C-2 and the other from the C-3-carbon of the propyl group [17]. Mechanistic proposals cover a sequential two-step reaction [18], a concerted reaction for isopropyl esters [19] or even an intermediate ion/molecule complex [20].

Therefore, these compounds offer the chance to determine both the formation enthalpy of the parent neutral ester and the proton affinity of the corresponding acid as well.

The relatively well investigated system of benzoic acid was chosen to confirm the applicability of this approach and the method is transferred to the nicotinic acid system.

The increase in the proton affinity from the benzoic core via the carbonyl group to the pyridinic core, as potential competing reaction centers, provides more insight into the fragmentation.

2. Experimental

Benzoic acid was obtained from Merck (Darmstadt). Benzoic acid *n*-butyl ester, nicotinic acid and nicotinic acid *n*-butyl ester were purchased from Aldrich. The samples were used as received. The measurements were performed with a Finnigan MAT95 mass spectrometer (Finnigan MAT, Bremen) with reversed Nier-Johnson geometry. Metastable ions were recorded in the two field-free regions between the ion acceleration and the magnetic sector field (FFR1) or between the magnetic sector and the electrostatic sector field (FFR2). Fragment ions of a selected parent ion, precursor ions of a selected fragment ion or parent ions which eliminate a specific neutral fragment were analyzed. The appropriate scan laws were set by the instrument.

Minimum energy thresholds for the formation of particular ions were obtained by extrapolating log (ion intensity) versus experimental electron energy to a vanishing ion intensity. A variety of references with masses and IEs or AEs close to the ion of investigation was used for the calibration of the energy scale: 1,2-dibromoethane (IE = 10.37 eV, AE ($C_2H_4Br^+$) = 10.53 eV), CH_2Br_2 (IE = 10.49 eV, AE (CH_2Br^+) = 11.25 eV), dibutylether (IE = 9.55 eV), benzene (IE = 9.244 eV), $CHCl_3$ (IE = 11.37 eV, AE ($CHCl_2^+$) = 11.57 eV, AE ($CHCl^+$) = 17.5 eV). All values were taken from Refs. [21] and [22]. For these experiments, the electron capture dynode was deactivated and the draw-out aperture was kept at the potential of the ionization chamber.

In this way, mass depending non-linearities in the ion transmission were corrected. Sample and reference ions were measured at the same particle density in the ionization chamber.

The sample temperatures were kept at 298 K with the exception of nicotinic acid, which was measured at a temperature of 330 K.

The results are summarized in Tables 1–4. The error limit reflects the actual spread in the obtained values.

3. Results and discussion

The following calculations of thermodynamic parameters uses a variety of necessary literature data, collected in Table 5. Derived thermochemical data are summarized in Table 8. Inher-

Table 1
Ionization and appearance energies of benzoic acid obtained on calibrated electron-impact ionization

m/z	IE, AE	Literature	Reference
122	9.47	9.66 (averaged)	[22,23], see text
105	11.17	11.5, 12.1, 12.11	[22,23]
77	13.94	14.3, 15.1, 15.08	[22,23]

All values are in eV. The error limit is ±0.3 eV.

Table 2
Ionization and appearance energies of benzoic acid *n*-butyl ester obtained on calibrated electron-impact ionization

m/z	IE, AE	Literature	Reference
178	9.43		
123	9.65		
122	10.79		
105	11.43	11.2 ± 0.1[a]	[23f]
79	11.96		
77	14.65	15.0 ± 0.03[a]	[23f]
56	10.67		

All values are in eV. The error limit is ±0.3 eV.

[a] Using Krypton as calibrant.

Table 3
Ionization and appearance energies of nicotinic acid obtained on calibrated electron-impact ionization

m/z	IE, AE	Literature	Reference
123	9.61	9.38	[24]
106	11.58		
105	10.94		
78	14.20		
77	13.67		

All values are in eV. The error limit is ±0.3 eV. The sum formula of the ions at *m/z* 78 ($C_5H_4N^+$) and *m/z* 77 ($C_5H_3N^{\bullet+}$) were confirmed by high resolution mass spectrometry.

ently, the enthalpies of formation of ions are derived according to the ion convention, which treats the electron as an ideal element in its standard state at all temperatures, arbitrarily setting its formation enthalpy $\Delta H_f^0(e^-) = 0$ [3].

Table 4
Ionization and appearance energies of nicotinic acid *n*-butyl ester obtained on calibrated electron-impact ionization

m/z	IE, AE
179	9.97
178	9.60
164	9.85
151	10.55
150	10.79
137	10.32
124	9.94
123	10.85
106	11.71
105	12.15
78	14.40
56	11.03

All values are in eV. The error limit is ±0.3 eV.

3.1. Benzoic acid (BA)

The mass spectrum of benzoic acid on EI ionization shows molecular ions $C_7H_6O_2^{\bullet+}$ at *m/z* 122. Their intensity is 95% of the base peak, which is characterized by $C_6H_5CO^+$ benzoyl ions at *m/z* 105. Other prominent fragments are $C_6H_5^+$ ions are at *m/z* 77 (90%) and $C_4H_3^+$ ions at *m/z* 51 (70%).

Thermochemical data of benzoic acid are crucial for the following evalution of benzoic acid *n*-butyl ester results. Literature data for ionization and appearance energies are scattered, even on application of the same ionization method. Published results for the ionization energy are IE = 9.3 eV (adiabatic) [22,23a], 9.41 eV (vertical) [23a], 9.6 eV [23b] on photoelectron spectroscopy and IE = (9.8 ± 0.2) eV [23c], 9.75 eV [23d] or (9.73 ± 0.09) eV [23e] on electron-impact ionization. From these data, an averaged value of IE = 9.66 eV is obtained for a vertical excitation. Even more scattered are the appearance energies for the $C_6H_5CO^+$ ion at *m/z* 105 on electron-impact ionization with AE (105^+) = (12.1 ± 0.1) eV [23c], 12.11 eV [23d] or (11.5 ± 0.07) eV [23f] and those for the $C_6H_5^+$ ion at *m/z* 77 with AE (77^+) = (15.1 ± 0.2) eV [23c], 15.08 eV [23d] or (14.3 ± 0.07) eV [23f].

Therefore, the ionization and appearance energies had to be remeasured and the results are listed in Table 1.

Using thermochemical data from Table 5, the appearance energy of $C_6H_5CO^+$ ions of AE (105^+) = (11.17 ± 0.3) eV is consistent with the calculated reaction enthalpy of $\Delta H_r = (11.45 \pm 0.2)$ eV according to reaction (1).

$$C_6H_5COOH \rightarrow C_6H_5CO^+ + HO^\bullet + e^- \qquad (1)$$

In addition, the AE (77^+) = (13.94 ± 0.3) eV is in good corroboration with $\Delta H_r = 14.11$ eV as obtained according to reaction (2).

$$C_6H_5COOH \rightarrow C_6H_5{}^+ + CO + HO^\bullet + e^- \qquad (2)$$

For a direct comparison with benzoic acid *n*-butyl ester, the metastable ion decay of benzoic acid was analyzed on chemical ionization using methane as reactant gas. Fragments of the quasi-molecular ion (MH^+), the $C_7H_7O_2^+$ ion at *m/z* 123, are $C_7H_6O_2^{\bullet+}$ ions at *m/z* 122. Furthermore, $C_7H_6O^{\bullet+}$ ions at *m/z* 106 and $C_7H_5O^+$ ions at *m/z* 105 are formed by elimination of $OH^\bullet$ or H_2O, respectively. $C_6H_7^+$ ions at *m/z* 79, formed by elimination of CO_2, are seen as their fragment ions and vice versa in the parent ion scan. Fragments of $C_7H_6O^{\bullet+}$ ions (*m/z* 106) are $C_7H_5O^+$ ions at *m/z* 105, $C_6H_6^{\bullet+}$ ions at *m/z* 78 and $C_6H_5^+$ ions at *m/z* 77. These results are very similar to the metastable ion decay of comparable ions of the corresponding ester.

3.2. Benzoic acid n-butyl ester (BABE)

A mass spectrum of benzoic acid butyl ester is presented in Fig. 1. Together with the analysis of the metastable ion decay (Table 6), a first insight into the fragmentation process is provided.

Molecular ions $C_{11}H_{14}O_2^{\bullet+}$ are seen at *m/z* 178. Fragment ions at *m/z* 149 and 135 are formed with very low intensity, espe-

Table 5
Gas-phase enthalpies of formation (ΔH_f^0), proton affinities (PA) and appearance energies

Species	Parameter	kJ/mol	eV	Reference
$H^\bullet$	ΔH_f^0	217.998	2.259	[21]
	IE		13.598	[21]
H^+	ΔH_f^0	1530	15.857	[21]
$HO^\bullet$	ΔH_f^0	38.99	0.404	[22]
H_2O	ΔH_f^0	−241.83	−2.506	[22]
CO	ΔH_f^0	−110	−1.15	[22]
CO_2	ΔH_f^0	−393.52	−4.079	[22]
$HOOC^\bullet$	ΔH_f^0	−223.0	−2.311	[22]
$C_6H_5{}^+$	ΔH_f^0	1138	11.794	[15]
$C_6H_7{}^+$	ΔH_f^0	862.53	8.9395	[15]
$C_6H_5CO^+$	ΔH_f^0	770.92	7.99 ± 0.2	[15]
$C_6H_5CO^\bullet$	ΔH_f^0	109.2 ± 8	1.13	[21]
Benzoic acid	ΔH_f^0	−295.2	−3.06	[22][a]
	IE		9.66 ± 0.3	[22,23][b]
	PA	821.1	8.51	[22]
	AE ($C_6H_5CO^+$)		11.90	[22,23][c]
Nicotinic acid	IE		9.38	[22,24]
	ΔH_f^0	−221.5 ± 1.5	−2.296	[22,25]
	PA	907	9.40	[26]
$C_4H_9O^\bullet$	ΔH_f^0	−62.8	−0.651	[21]
C_4H_8				
1-Butene	ΔH_f^0	−0.63 ± 0.79	−0.006	[21,22]
	IE		9.55	[21,22]
$C_4H_7{}^\bullet$				
$MeCH{=}CH{-}C^\bullet H_2$	ΔH_f^0	125.5 ± 6.3	1.30	[21]
$H_2C{=}CHC^\bullet HMe$	ΔH_f^0	125.5 ± 6.3	1.30	[21]
$H_2C{=}CHCH_2C^\bullet H_2$	ΔH_f^0	192.5	2.00	[27]
Cyclobutyl	ΔH_f^0	214.2 ± 4.2	2.22	[21]
Cyclopropylmethyl	ΔH_f^0	213.8 ± 6.7	2.22	[21]
$EtC^\bullet{=}CH_2$	ΔH_f^0	246.8	2.56	Estimated [d]
Benzene	IE		9.244	[22]
	PA	750.4	7.78	[22]
Pyridine	IE		9.26	[22]
	PA	930	9.64	[22]
3-Acetopyridine	PA	916.2	9.50	[22]

[a] ΔH_f^0 (g) was calculated from $\Delta H_f^0(s) = -3.988$ eV and ΔH^0 (sub) = (0.922 ± 0.04) eV [22].
[b] Mean value from IE (eV, PES) = 9.41, 9.60; IE (eV, EI) = 9.80, 9.75, 9.73.
[c] Mean value from AE (eV) = 12.1, 12.11, 11.5.
[d] Estimated from ΔH_f^0 (1-butene) and D(C—H) = 465.3 kJ/mol for ethylene [27].

cially in comparison with nicotinic acid butyl ester (see below), by elimination of $C_2H_5{}^\bullet$ or $C_3H_7{}^\bullet$, respectively. The dominant fragmentation process, however, is the elimination of $C_4H_7{}^\bullet$ radicals yielding the prominent $C_7H_7O_2{}^+$ ions at *m/z* 123. These $C_7H_7O_2{}^+$ ions are precursors for three further fragment ions, $C_7H_6O^{\bullet+}$ (*m/z* 106) by elimination of $OH^\bullet$, $C_7H_5O^+$ (*m/z* 105) by elimination of H_2O or $C_6H_7{}^+$ (*m/z* 79) by elimination of CO_2.

$C_7H_6O_2{}^{\bullet+}$ ions at *m/z* 122 are formed from molecular ions by loss of C_4H_8 (1-butene). Subsequent elimination of $OH^\bullet$ radicals leads to $C_7H_5O^+$ ions at *m/z* 105. $C_6H_7{}^+$ ions at *m/z* 79, as metastable fragments, were observed only in the fragment ion scan in FFR1. Due to its absence in FFR2, this peak is regarded as an artefact, most probably induced from an interfering decay from the more intensive $C_7H_7O_2{}^+$ ions at *m/z* 123.

$C_7H_5O^+$ ions at *m/z* 105 eliminate CO thus forming $C_6H_5{}^+$ ions at *m/z* 77.

$C_4H_8{}^{\bullet+}$ ions at *m/z* 56 are directly produced from parent molecular ions by elimination of neutral benzoic acid.

A more detailed insight into these various fragmentation steps is achieved by a thermochemical analysis.

The formation enthalpy of benzoic acid butyl ester is derived from two pathways, summarized by reactions (3) and (4). Both pathways represent the classical McLafferty rearrangement and the detailed mechanism is disputed between a concerted or a stepwise reaction via an intermediate distonic ion [28].

$$\text{BABE} \rightarrow \text{BA}^{\bullet+} + C_4H_8 + e^- \qquad (3)$$

or

$$\text{BABE} \rightarrow \text{BA} + C_4H_8{}^{\bullet+} + e^- \qquad (4)$$

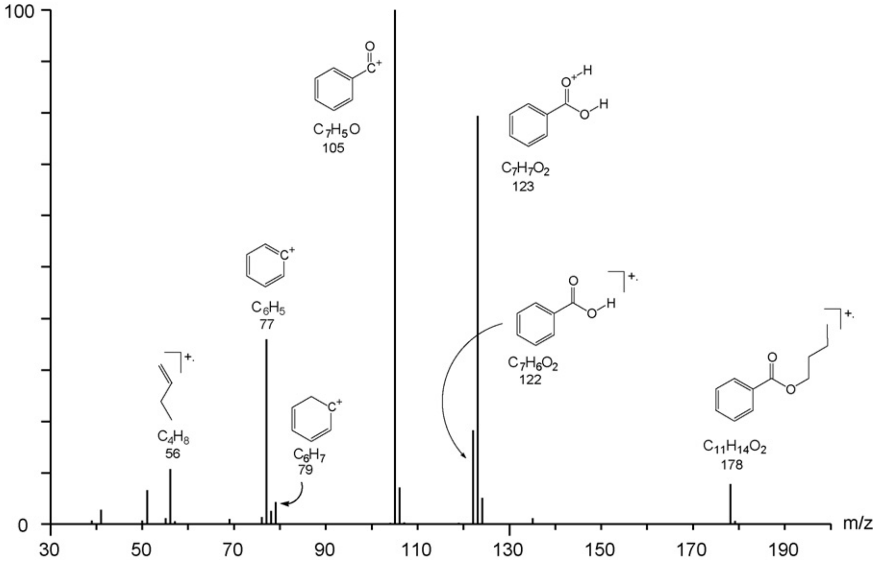

Fig. 1. Mass spectrum of benzoic acid *n*-butyl ester on EI ionization at 70 eV.

Table 6
Metastable ion decay of benzoic acid *n*-butyl ester on electron-impact ionization (electron energy: 70 eV)

(a) Fragment ions of a given parent ion

Parent ions	m/z	Fragment ions	m/z	Relat. intensity (%)
$C_{11}H_{14}O_2^{\bullet+}$	178	$C_7H_7O_2^+$	123	Strong
$C_7H_7O_2^+$	123	$C_7H_6O_2^{\bullet+}$	122	5
		$C_7H_6O^{\bullet+}$	106	20
		$C_7H_5O^+$	105	45
		$C_6H_7^+$	79	100, strong
$C_7H_6O_2^{\bullet+}$	122	$C_7H_5O^+$	105	
		$C_6H_7^+$	79	Artefact in FFR1
$C_7H_5O^+$	105	$C_6H_5^+$	77	
$C_6H_7^+$	79	$C_6H_5^+$	77	

(b) Parent ions of a given fragment ion

Fragment ions	m/z	Parent ions	m/z	Relat. intensity (%)
$C_4H_8^{\bullet+}$	56	$C_{11}H_{14}O_2^{\bullet+}$	178	Tiny
$C_6H_5^+$	77	$C_6H_7^+$	79	
		$C_7H_5O^+$	105	Strong
$C_6H_7^+$	79	$C_7H_7O_2^+$	123	
$C_7H_5O^+$	105	$C_7H_6O_2^{\bullet+}$	122	
		$C_9H_9O_2^+$	149	
$C_7H_6O_2^{\bullet+}$	122	$C_{11}H_{14}O_2^{\bullet+}$	178	
$C_7H_7O_2^+$	123	$C_{11}H_{14}O_2^{\bullet+}$	178	

(c) Precursor ions eliminating a neutral fragment of specific mass

Neutral	Mass	Parent ions	m/z
H_2O	18	$C_7H_7O_2^+$	123
CO_2	44	$C_7H_7O_2^+$	123
$C_4H_7^\bullet$	55	$C_{11}H_{14}O_2^{\bullet+}$	178

As depicted in Fig. 2, reactions (3) and (4) differ only in the distribution of the positive charge among the two products. Since the IEs of 1-butene and BABE are in a comparable range (Tables 2 and 5), the charge distribution among both is in agreement with the semi-empirical rule of Stevenson.

According to reaction (3), the AE ($BA^{\bullet+}$) of 10.79 eV and the formation enthalpies of $BA^{\bullet+}$ and 1-butene yields a formation enthalpy of BABE of −4.386 eV.

It should be kept in mind, that this result is directly dependent on the ionization energy of benzoic acid.

According to reaction (4), the AE ($C_4H_8^{\bullet+}$) of 10.67 eV and the formation enthalpies of benzoic acid and the 1-butene cation $C_4H_8^{\bullet+}$ a formation enthalpy of BABE of −4.186 eV is obtained.

From both results, a mean value for the formation enthalpy of $\Delta H_f^0\,(\mathrm{BABE}) = (-4.286 \pm 0.3)$ eV is calculated, equivalent to (-414 ± 30) kJ/mol (Table 8).

If an activation energy for the H-transfer must be taken into account, the experimental appearance energies for the product ions would be higher than the pure thermochemical reaction enthalpy by the same amount. The same holds for the derived formation enthalpies.

The contribution of a potential activation energy is estimated from the dissociation energy (*D*) of benzoic acid or benzoic acid butyl ester to a benzoyl radical and their counter radicals according to reactions (5) and (6).

$$\mathrm{BA} \rightarrow C_6H_5CO^\bullet + HO^\bullet \quad (5)$$

$$\mathrm{BABE} \rightarrow C_6H_5CO^\bullet + C_4H_9O^\bullet \quad (6)$$

For benzoic acid $D = 4.59$ eV is calculated (data from Table 5), which is in good correlation to $D = 4.76$ eV for BABE. This result points to an insignificant activation energy for the H-transfer during the McLafferty rearrangement.

The ion at *m*/*z* 123 represents a protonated form BAH^+ of benzoic acid. A sequential reaction mechanism for the involved double H-transfer is depicted in Fig. 3. Previously, a mechanis-

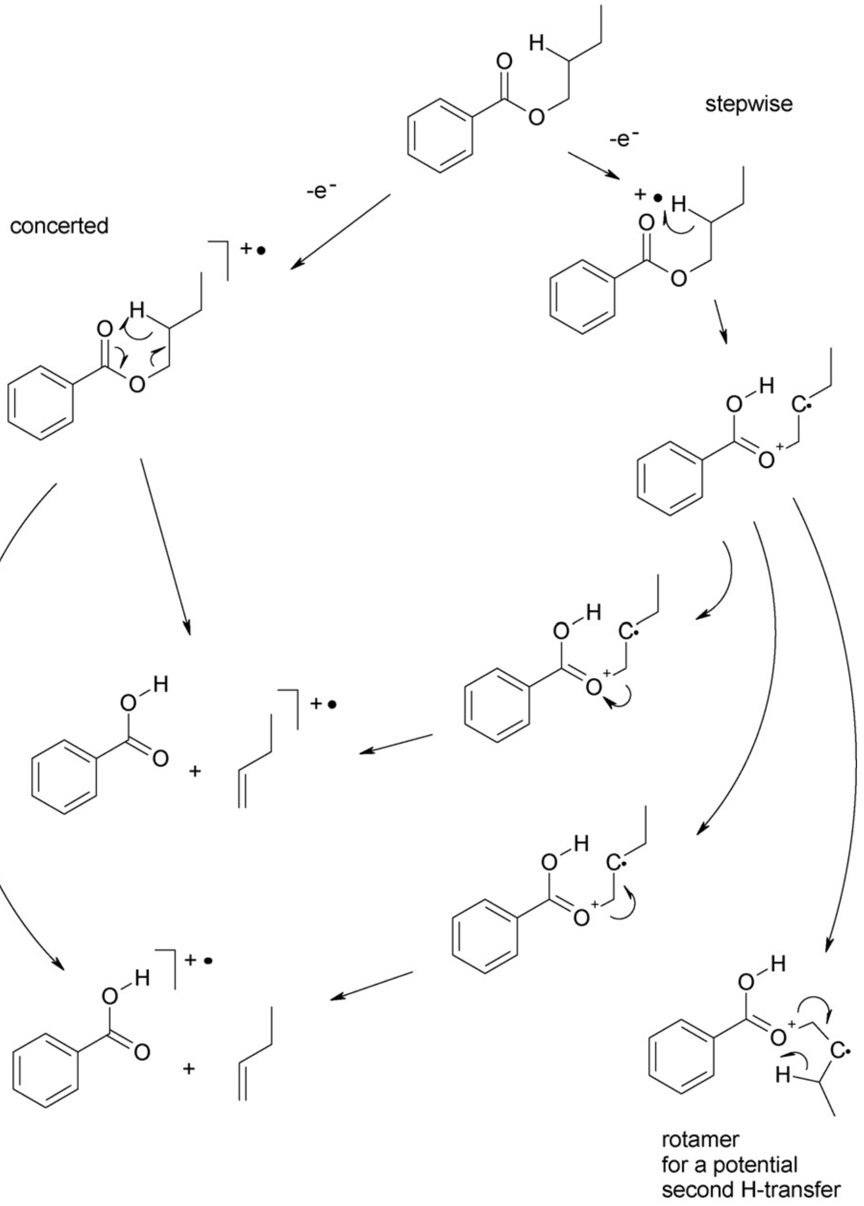

Fig. 2. McLafferty rearrangement of benzoic acid *n*-butyl ester: a concerted and a stepwise reaction mechanism.

tic proposal has been published for *n*-propyl esters by Benoit et al. [18]. According to this, the first step, a single H-transfer from the 2-alkyl position to the carbonyl oxygen, is exothermic, apparently occuring without activation energy. This provides the internal excess energy for the subsequent rearrangement and fragmentation, being endothermic by roughly the same amount. Additionally, by appearance energy measurements, the protonation site of carboxylic acids has been shown to be the carbonyl group rather than the OH group [18].

Among the two distinct structures of $C_4H_7^{\bullet}$ radicals in Fig. 3, preference is given to the methylallyl radical formed via reactions (a) and (b). At energetic threshold conditions, the alternatives, including a cyclopropylmethyl or a cyclobutyl radical, are ruled out by their high formation enthalpies. The same holds for the $EtC^{\bullet}=CH_2$ radical which may be formed in a four-membered transition state (Table 5). As depicted in Figs. 2 and 3, the stepwise mechanism for the single H-transfer could easily explain the competing double H-transfer by the formation of a rotamer.

According to reaction (7), the AE $(123^+) = 9.65$ eV and the formation enthalpy of the methylallyl $C_4H_7^{\bullet}$ radical a formation enthalpy of the BAH^+ ion of (4.064 ± 0.3) eV is obtained.

$$\mathrm{BABE} \rightarrow \mathrm{BAH}^+ + C_4H_7^{\bullet} + e^- \qquad (7)$$

This formation enthalpy of BAH^+ is interpreted according to reaction (8).

$$\mathrm{BAH}^+ \rightarrow \mathrm{BA} + H^+ \qquad (8)$$

Using formation enthalpies of benzoic acid and H^+ (Table 5), a reaction (8) enthalpy of $\Delta H_r = (8.73 \pm 0.3)$ eV is obtained. This reaction enthalpy corresponds to the proton affinity of ben-

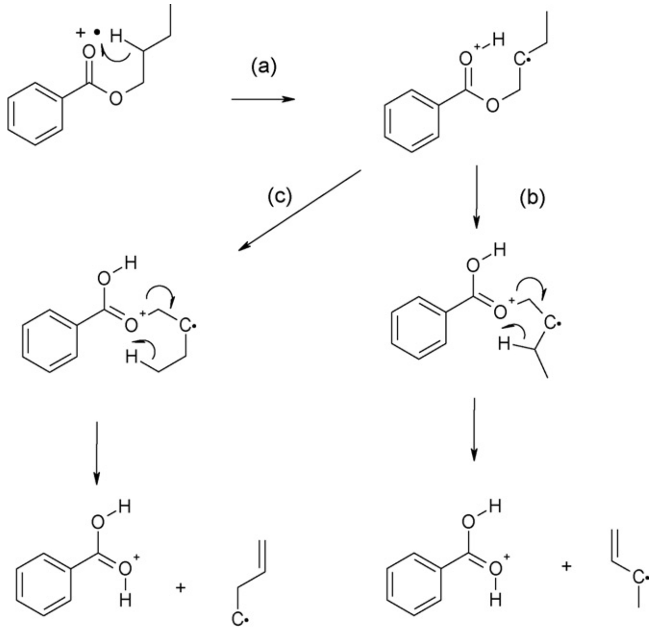

Fig. 3. A sequential charge-controlled mechanism for the transfer of two H-atoms leading to the formation of a protonated acid.

zoic acid as derived from appearance energy data. Within the experimental error of the AE determinations and the underlying literature data of benzoic acid, this result agrees well with a published proton affinity of PA = 8.51 eV (Table 5). Therefore, with good evidence, the described reactions are occuring near to their thermochemical enthalpies. Activation energy barriers for the two reactions (a) the transfer of either one H-atom during the McLafferty rearrangement (used for the calculation of the parent formation enthalpy) and (b) the transfer of two H-atoms leading to the protonated intermediate (used for the calculation of the proton affinity of benzoic acid) are insignificant. This is supported by comparison with mandelic acid and its methyl ester on EI ionization, where fragmentation to molecular products, involving the intramolecular transfer of one H-atom, was found to occur without significant internal excess energy [15]. Furthermore, this result is characteristic for the thermochemically favoured protonation of the carbonyl group rather than the phenyl core as compared with PA = 7.78 eV for benzene [22].

Confirmed by the metastable ion analysis, the next fragment ion of BABE, $C_6H_5CO^+$ ions at *m/z* 105, can be formed by three different processes.

The first represents a direct α-cleavage according to reaction (9).

$$\text{BABE} \rightarrow C_6H_5CO^+ + C_4H_9O^\bullet + e^- \qquad (9)$$

A reaction enthalpy of $\Delta H_r = (11.63 \pm 0.2)$ eV is calculated.

The second formation process (10) is the elimination of H_2O from the intermediate protonated acid (BAH^+).

$$C_7H_7O_2{}^+ \rightarrow C_6H_5CO^+ + H_2O \qquad (10)$$

From BABE, an overall thermochemical reaction enthalpy of $\Delta H_r = (11.07 \pm 0.2)$ eV is calculated. The experimental AE $(105^+) = (11.43 \pm 0.3)$ eV is in accordance with both processes. With respect to the appearance energy of the $C_6H_5{}^+$ ions (as products by CO elimination) and the results for nicotinic acid butyl ester, which point to the need of an activation energy for this elimination (see below), preference is given to reaction (9).

The third option, a formation via intermediate benzoic acid ions and subsequent elimination of $OH^\bullet$ radicals, needs a thermochemical reaction enthalpy of $\Delta H_r = 12.67$ eV and can definitely be ruled out at energetic threshold conditions.

Benzoyl cations $C_6H_5CO^+$ are prominent, but not the only, precursors for $C_6H_5{}^+$ ions at *m/z* 77.

The first pathway to $C_6H_5{}^+$ ions is the elimination of CO from these benzoyl ions according to reaction (11).

$$C_6H_5CO^+ \rightarrow C_6H_5{}^+ + CO \qquad (11)$$

Within the experimental error limit, the difference between AE (77^+) and AE (105^+) of 3.22 eV is in acceptable corroboration with the calculated thermochemical reaction enthalpy of $\Delta H_r = (2.66 \pm 0.2)$ eV. The reason for the apparent discrepancy seems to be the relatively low AE (105^+). From BABE, the overall fragmentation via reaction (12) comprises only simple bond cleavages, which predominantly fulfill the requirement to occur without additional activation energy [4].

$$\text{BABE} \rightarrow C_6H_5{}^+ + CO + C_4H_9O^\bullet + e^- \qquad (12)$$

A thermochemical reaction enthalpy of 14.28 eV is obtained which is in fairly good corroboration with the experimental result of AE $(77^+) = (14.65 \pm 0.3)$ eV.

The second pathway to $C_6H_5{}^+$ ions includes the last prominent fragment ion, $C_6H_7{}^+$ at *m/z* 79. As seen in the metastable ion decay of protonated benzoic acid and its butyl ester, this ion is formed from BAH^+ ions according to

$$C_7H_7O_2{}^+ \rightarrow C_6H_7{}^+ + CO_2 \qquad (13)$$

A thermochemical reaction (13) enthalpy of $\Delta H_r = 0.80$ eV is calculated. Therefore, based on the AE $(123^+) = 9.65$ eV, an appearance energy of 10.45 eV is expected for the $C_6H_7{}^+$ ion. The comparison with the experimental value of AE $(79^+) = 11.96$ eV points to an activation energy of 1.51 eV for this elimination process, which involves the transfer of two H-atoms to the phenyl core during the elimination of CO_2. A very similar behaviour has been found for the elimination of CO from protonated benzaldehyde with an activation energy of (1.1 ± 0.1) eV [15]. $C_6H_7{}^+$ ions are known precursors for $C_6H_5{}^+$ ions. A thermochemical reaction enthalpy of $\Delta H_r = 2.86$ eV has been calculated for the elimination of H_2 and an activation energy of (1.1 ± 0.1) eV was assigned to this process [15]. Concerning the decay of protonated benzoic acid, this acquired excess energy will be distributed among the $C_6H_7{}^+$ ions and CO_2, since a significant intermolecular collision-induced energy dissipation is not likely under the experimental conditions for the determination of the appearance energies. Being a better acceptor of internal excess energy than CO, CO_2 may be a significant shareholder of the previously acquired activation energy of 1.51 eV. For $C_6H_5{}^+$ ions, formed on this pathway, an appearance energy between 14.42 and 15.92 eV is expected, depending on the shared internal excess energy of the $C_6H_7{}^+$ ions and its

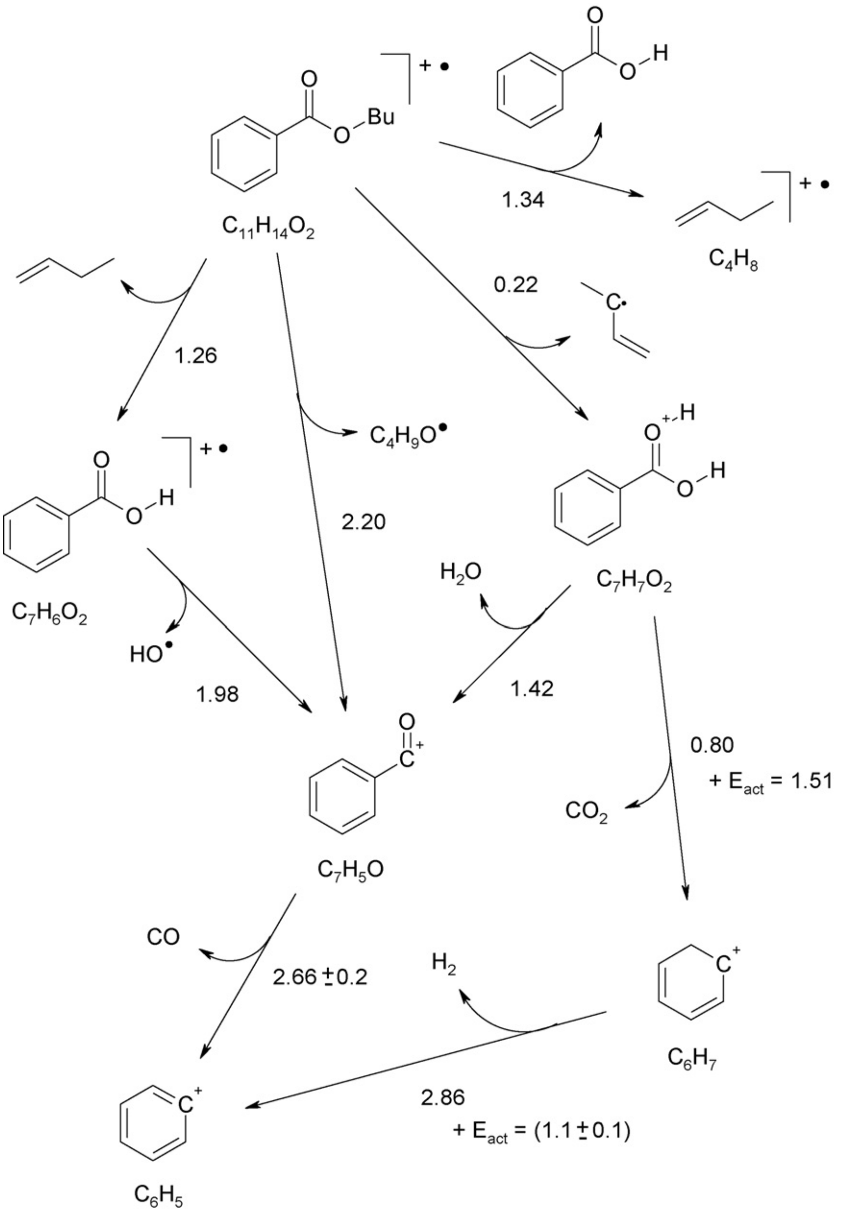

Fig. 4. Derived thermochemical reaction enthalpies and activation energies E_{act} (in eV) for the fragmentation of benzoic acid *n*-butyl ester.

distribution (Fig. 4). Therefore, this route is more endothermic than reaction (12).

In view of the various pathways to $C_6H_5^+$ ions (and to $C_6H_5CO^+$ ions as well) near to the energetic threshold conditions, some differences between the experimental AEs and calculated reaction enthalpies may be caused by the vanishing ion extrapolation method itself, since, with slightly increased electron energies, additional pathways are accessible and will influence the ion intensity.

3.3. *Nicotinic acid (NA)*

A mass spectrum is shown in Fig. 5. On EI ionization, the metastable ion analysis revealed molecular ions $C_6H_5NO_2^{\bullet+}$ at *m*/*z* 123 as precursors of $C_6H_3NO^{\bullet+}$ ions at *m*/*z* 105. Remarkably, $C_6H_4NO^+$ ions (*m*/*z* 106), as fragments by $OH^\bullet$ elimination, were not detected. In the precursor scan of $C_6H_4NO^+$ ions only the low abundant $(M+1)^+$ peak was observed, which points to an actually monitored transition from the ^{13}C isotope peak of molecular ions. $C_6H_4NO^+$ ions at *m*/*z* 106 are precursors of $C_6H_3NO^{\bullet+}$ ions (*m*/*z* 105) and $C_5H_4N^+$ ions (*m*/*z* 78). $C_6H_3NO^{\bullet+}$ ions at *m*/*z* 105 are precursors of $C_5H_3N^{\bullet+}$ ions (*m*/*z* 77).

On chemical ionization using methane as reactant gas, the fragmentation of the $C_6H_6NO_2^+$ (MH^+) ion at *m*/*z* 124 was governed by $C_6H_5NO_2^{\bullet+}$ ions (*m*/*z* 123), $C_6H_4NO^+$ (*m*/*z* 106) and $C_5H_6N^+$ ions (*m*/*z* 80), $C_5H_5N^{\bullet+}$ ions (*m*/*z* 79) and $C_5H_4N^+$ ions (*m*/*z* 78). Prior to the discussion of nicotinic acid butyl ester, relevant formation enthalpies for common intermediate ions are derived. In this case, the slightly enhanced sample temperature of 330 K does not significantly affect the given ΔH_f^0 values since the integrated heat capacity between 298 and 330 K is regarded

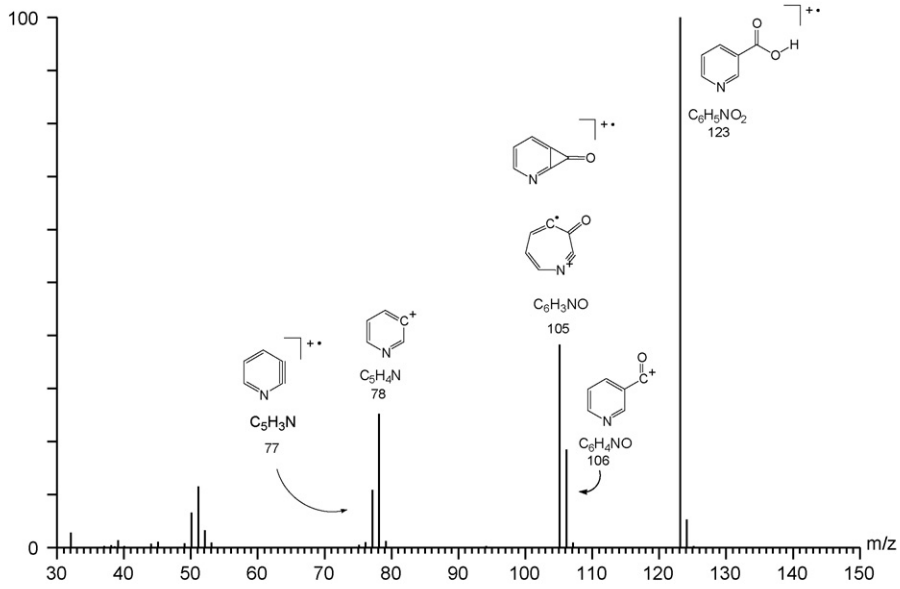

Fig. 5. Mass spectrum of nicotinic acid on EI ionization at 70 eV.

to be far below the experimental error limit in the determination of the appearance energies.

The formation enthalpy of the $C_6H_4NO^+$ cation is calculated from the AE (106^+) = 11.58 eV and the formation enthalpy of the $OH^\bullet$ radical (Tables 3 and 5) according to the α-cleavage reaction (14).

$$\mathrm{NA} \rightarrow C_6H_4NO^+ + HO^\bullet + e^- \quad (14)$$

A value of ΔH_f^0 ($C_6H_4NO^+$) = 8.88 eV is obtained.

This is in a reasonable correlation with ΔH_f^0 ($C_6H_5CO^+$) = 7.99 eV for the benzoyl cation with a difference of $\Delta\Delta H_f^0$ = 0.89 eV between the two enthalpies of formation. Continuing the fragmentation by elimination of CO from $C_6H_4NO^+$ ions to $C_5H_4N^+$ ions, the formation enthalpy $\Delta H_f^0(C_5H_4N^+)$ = 12.65 eV is calculated from its AE (78^+) = 14.20 eV according to reaction (15).

$$\mathrm{NA} \rightarrow C_5H_4N^+ + CO + HO^\bullet + e^- \quad (15)$$

Again, this result is in a reasonable correlation with $\Delta H_f^0(C_6H_5{}^+) = 11.794$ eV with a difference of $\Delta\Delta H_f^0$ = 0.86 eV.

Furthermore, a $\Delta H_f^0(C_5H_4N^\bullet)$ = 4.05 eV (391.0 kJ/mol for pyrid-3-yl [27]) leads to IE ($C_5H_4N^\bullet$) = 8.60 eV in good correlation to IE ($C_6H_5{}^\bullet$) = 8.39 eV.

The abundant formation of the fragment ion at *m/z* 105 is unparalleled by benzoic acid. Since the AE (105^+) is lower than AE (106^+), the formation is interpreted with an elimination of H_2O from the molecular ion.

$$\mathrm{NA} \rightarrow C_6H_3NO^{\bullet+} + H_2O + e^- \quad (16)$$

Since intensive fragment ions at *m/z* 105 are specific for the 3-pyridinecarboxylic acid, α-cleavage of the 2-pyridine-hydrogen is the most likely step for its formation. This is supported by a study using site-specifically deuterated analogs of nicotinic acid [29].

With respect to a potential activation energy for this process, an upper limit for the formation enthalpy of $\Delta H_f^0(C_6H_3NO^+)$ = 11.15 eV is derived using the AE (105^+) = 10.94 eV.

It may be speculated that the dominance of this fragment ion is caused by a ring opening to a thermochemically favoured ion with a seven-ring cyclic structure. $C_5H_3N^{\bullet+}$ ions at *m/z* 77 are formed by subsequent elimination of CO. Its structure is assigned to that of 2,3-didehydropyridine. An upper limit of ΔH_f^0 = 15.03 eV is derived for this ion. Some data for benzyne are available for comparison. An early work reports an ionization energy of 9.75 eV and a formation enthalpy of ΔH_f^0 = 5.12 eV [30a]. More recent results point to a lower ΔH_f^0 = 5.08 eV [30b] or 4.56 eV [30c,d] and (on PES) to IE = 9.24 eV [30e] or 9.03 eV [30f]. On average, a ΔH_f^0 (C_6H_4) = (4.82 ± 0.3) eV and IE = (9.15 ± 0.1) eV lead to ΔH_f^0 ($C_6H_4{}^{\bullet+}$) = 13.97 eV with a reasonable difference of $\Delta\Delta H_f^0 \approx 1$ eV to $C_5H_3N^{\bullet+}$. Therefore, potential activation barriers should not exceed the given error limit.

3.4. Nicotinic acid n-butyl ester (NABE)

Molecular ions $C_{10}H_{13}NO_2{}^{\bullet+}$ are seen at *m/z* 179 in the mass spectrum (Fig. 6). Documented by their metastable ion decay, they are direct precursors of fragment ions at *m/z* 178, 164, 151, 150 and 137. These five fragment ions are formed by elimination of $H^\bullet$, $CH_3{}^\bullet$, C_2H_4, $C_2H_5{}^\bullet$ or C_3H_6, respectively. A comparable elimination is virtually absent for benzoic acid *n*-butyl ester. Similar fragmentations are seen in many pyridine compounds with long aliphatic chains. In correlation with the significantly increased proton affinity of the pyridine core in comparison to the benzene core, this behaviour is rationalized as being caused by an increased cation affinity. Therefore, it is concluded that the cationic fragment ions are stabilized by interfering (in any form of a cyclisation) with the pyridine core. The structure of the radical cations at *m/z* 151 and 137 is

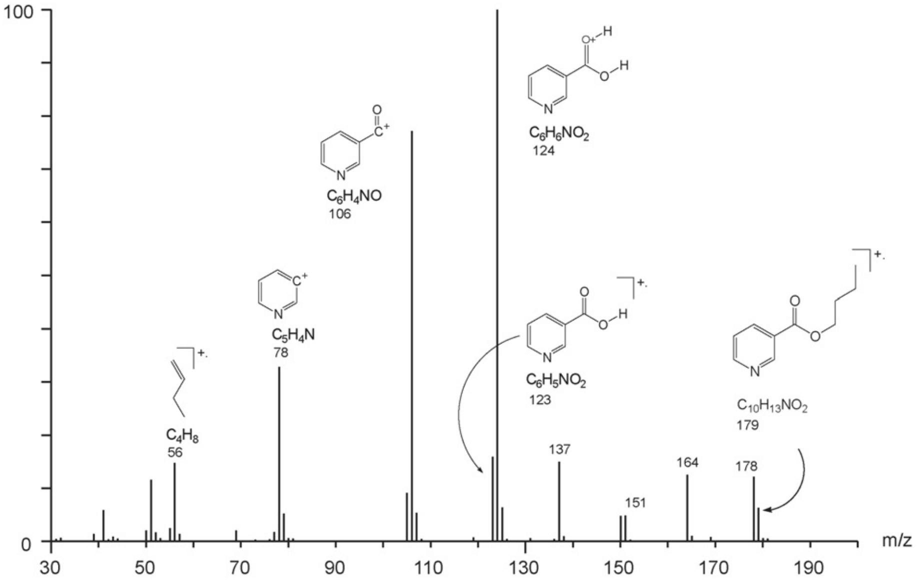

Fig. 6. Mass spectrum of nicotinic acid *n*-butyl ester on EI ionization at 70 eV. See discussion of the protonation site for the $C_6H_6NO_2^+$ ion at *m/z* 124.

tentatively assigned to the ethyl and the methyl ester, respectively.

The dominant fragmentation of molecular ions, however, is the elimination of $C_4H_7^\bullet$ radicals leading to $C_6H_6NO_2^+$ ions at *m/z* 124 (Table 7). This ion represents a protonated form of nicotinic acid, where the actual protonation site could be either the pyridine core or, as in the case of benzoic acid, the carbonyl group. From these $C_6H_6NO_2^+$ ions, a sequential elimination of H_2O and CO leads to $C_6H_4NO^+$ ions at *m/z* 106 and to $C_5H_4N^+$ ions at *m/z* 78, respectively. In addition, a direct formation of $C_5H_4N^+$ ion from these precursors points to a contribution of a fast elimination of H_2O and CO or to an elimination of CH_2O_2. With low abundance, $C_5H_6N^+$ ions at *m/z* 80 are formed by the metastable elimination of CO_2 from parent $C_6H_6NO_2^+$ ions.

The second important fragmentation pathway from molecular ions is a classical McLafferty rearrangement leading to $C_6H_5NO_2^{\bullet+}$ ions at *m/z* 123 by elimination of C_4H_8 (1-butene). The subsequent fragmentation is similar to the pure nicotinic acid and involves the elimination of either H_2O yielding $C_6H_3NO^{\bullet+}$ ions (*m/z* 105) or a sequential elimination of $OH^\bullet$ and CO yielding $C_6H_4NO^+$ ions (*m/z* 106) and $C_5H_4N^+$ ions (*m/z* 78), respectively.

1-Butene $C_4H_8^{\bullet+}$ ions at *m/z* 56 are directly formed from molecular ions by elimination of neutral nicotinic acid.

A more detailed insight is achieved in conjunction with thermochemical data (Fig. 7).

In analogy to BABE, the formation enthalpy of NABE is derived from two reaction pathways.

$$\mathrm{NABE} \rightarrow \mathrm{NA}^{\bullet+} + C_4H_8 + e^- \tag{17}$$

or

$$\mathrm{NABE} \rightarrow \mathrm{NA} + C_4H_8^{\bullet+} + e^- \tag{18}$$

According to reaction (17) or reaction (18) and published data from Table 5, formation enthalpies of −3.542 eV or −3.782 eV are obtained, respectively. Supported by the results for BABE, an insignificant activation energy for the involved H-transfer is assumed. Thus, a mean value for the formation enthalpy of $\Delta H_f^0\,(\mathrm{NABE}) = (-3.662 \pm 0.3)\,\mathrm{eV}$ is obtained, equivalent to (-353 ± 30) kJ/mol (Table 8).

The appearance energy of the $C_6H_6NO_2^+$ ion at *m/z* 124, representing a protonated form of nicotinic acid (NAH^+), allows the calculation of a proton affinity of this acid.

Its formation is summarized according to

$$\mathrm{NABE} \rightarrow C_6H_6NO_2^{\ +} + C_4H_7^\bullet + e^- \tag{19}$$

At this point, the formation enthalpy of the $C_4H_7^\bullet$ radical and its structure is a crucial parameter. Following the discussion for BABE (see Fig. 3), at energetic threshold conditions preference is given to the $C_4H_7^\bullet$ methylallyl radical over the alternative structures.

From the appearance energy AE (124^+) = 9.94 eV, a formation enthalpy for this $C_6H_6NO_2^+$ ion of 4.978 eV is calculated.

Using this value and additional data from Table 5, a reaction enthalpy of 8.58 eV is calculated according to

$$\mathrm{NAH}^+ \rightarrow \mathrm{NA} + \mathrm{H}^+ \tag{20}$$

The enthalpy for this reaction corresponds directly to the proton affinity of nicotinic acid and a value of PA (NA) = 8.58 eV (≡828 kJ/mol) is obtained.

The result is very similar to the result for a protonation of the carbonyl group of benzoic acid (Table 5). On the other hand, however, the discrepancy to a published proton affinity of PA = 9.40 eV [26], measured by the kinetic method, and well-known proton affinities of various pyridine compounds for a protonation of the pyridinic nitrogen of roughly 9.5 eV (e.g., 3-acetopyridine, Table 5) is striking. A tentative decision between these two protonation sites is based on the following arguments.

Underlying a protonation at the pyridinic nitrogen with a proton affinity of 9.40 eV for nicotinic acid, a formation enthalpy

Table 7
Metastable ion decay of nicotinic acid *n*-butyl ester on electron-impact ionization (electron energy: 70 eV)

(a) Fragment ions of a given parent ion

Parent ions	*m/z*	Fragment ions	*m/z*	Relat. intensity (%)
$C_{10}H_{13}NO_2^{\bullet +}$	179	$C_{10}H_{12}NO_2^+$	178	100
		$C_9H_{10}NO_2^+$	164	15
		$C_8H_9NO_2^{\bullet +}$	151	3
		$C_8H_8NO_2^+$	150	2
		$C_7H_7NO_2^{\bullet +}$	137	12
		$C_6H_6NO_2^+$	124	60
$C_6H_6NO_2^+$	124	$C_6H_5NO_2^{\bullet +}$	123	15
		$C_6H_4NO^+$	106	100, strong
		$C_6H_3NO^{\bullet +}$	105	20
		$C_5H_6N^+$	80	5
		$C_5H_4N^+$	78	5
$C_6H_5NO_2^{\bullet +}$	123	$C_6H_4NO^+$	106	3
		$C_6H_3NO^{\bullet +}$	105	100, strong
$C_6H_4NO^+$	106	$C_6H_3NO^{\bullet +}$	105	40
		$C_5H_4N^+$	78	100, strong
$C_6H_3NO^{\bullet +}$	105	$C_5H_4N^+$	78	15
		$C_5H_3N^{\bullet +}$	77	100

(b) Parent ions of a given fragment ion

Fragment ions	*m/z*	Parent ions	*m/z*	Relat. intensity (%)
$C_4H_8^{\bullet +}$	56	$C_{10}H_{13}NO_2^{\bullet +}$	179	Tiny
$C_5H_4N^+$	78	$C_6H_4NO^+$	106	
		$C_6H_6NO_2^+$	124	
$C_6H_3NO^{\bullet +}$	105	$C_6H_4NO^+$	106	
		$C_6H_5NO_2^{\bullet +}$	123	
$C_6H_4NO^+$	106	$C_6H_6NO_2^+$	124	
		$C_{10}H_{13}NO_2^{\bullet +}$	179	
$C_6H_5NO_2^{\bullet +}$	123	$C_8H_9NO_2^{\bullet +}$	151	
		$C_{10}H_{13}NO_2^{\bullet +}$	179	
$C_6H_6NO_2^+$	124	$C_{10}H_{13}NO_2^{\bullet +}$	179	Strong
$C_7H_7NO_2^{\bullet +}$	137	$C_{10}H_{13}NO_2^{\bullet +}$	179	
$C_8H_9NO_2^{\bullet +}$	151	$C_{10}H_{13}NO_2^{\bullet +}$	179	
$C_9H_{10}NO_2^+$	164	$C_{10}H_{13}NO_2^{\bullet +}$	179	

Table 8
Derived gas-phase enthalpies of formation (ΔH_f^0) and proton affinities (PA)

Species	Parameter	eV	kJ/mol
$C_6H_4NO^+$	ΔH_f^0	8.88[a]	857
$C_6H_3NO^{\bullet +}$	ΔH_f^0	11.15	1076
$C_5H_4N^+$	ΔH_f^0	12.65[b]	1221
$C_5H_3N^{\bullet +}$	ΔH_f^0	15.03[c]	1450
$BA^{\bullet +}$	ΔH_f^0	6.41	618
BAH^+	ΔH_f^0	4.064	392
NAH^+	ΔH_f^0	4.978	480
NA	PA	8.58[d]	828
BABE	ΔH_f^0	−4.286	−414
$BABE^{\bullet +}$	ΔH_f^0	5.144	496
NABE	ΔH_f^0	−3.662	−353
$NABE^{\bullet +}$	ΔH_f^0	6.308	609

The estimated error is ±0.3 eV (±30 kJ/mol).

[a] Compare with $\Delta H_f^0(C_6H_5CO^+) = (7.99 \pm 0.2)$ eV.

[b] Compare with $\Delta H_f^0(C_6H_5^+) = 11.794$ eV.

[c] Structure assigned to 2,3-didehydropyridine.

[d] For a protonation of the carbonyl group.

of NAH^+ of 4.16 eV is anticipated. Retrospectively, the appearance energy for the protonated acid of AE $(124^+) = 9.94$ eV for reaction (19) is thermochemically in accordance with a formation enthalpy of 2.12 eV for the $C_4H_7^\bullet$ radical. The choice of corresponding candidates, listed in Table 5, would imply a fragmentation mechanism totally different to that of benzoic acid butyl ester. However, concerning the formation of protonated acids, literature mass spectra reveal a common behaviour of esters of both acids, depending only on the length of the ester chain. The fragmentation of ethyl esters is dominated by a classical McLafferty rearrangement leading to the organic acids. Protonated acids (by a formal elimination of a $C_2H_3^\bullet$ radical) are not observed. In contrast to this, the intermediate formation of protonated acids starts with propyl esters. Their abundance dominates over ions of the corresponding acid, even for isopropyl esters. Emphasized in the last case, both esters show a parallel fragmentation in respect of the absence of additional fragment ions for the nicotinic acid ester. One aspect for the competitive transfer of a second H-atom over the alken loss could be the formation of a rotamer allowing the abstraction from a saturated CH_3 group instead of that from a radicalic CH_2 end group for ethyl esters.

A further argument supports the assumption of a protonated carbonyl group: the difference of the PA values for the N-protonated and the CO-protonated form of $\Delta PA = 0.82$ eV is in accordance with a density functional theory (DFT) molecular orbital approach, where, e.g., for 2-aminonicotinic acid, the nicotinic-N-protonated form was found to be more stable than the carbonyl-protonated form by 1.12 eV. In addition, a proton affinity of 9.51 eV was obtained for the formation of the N-protonated nicotinic acid [31]. Following this method, we reproduced this value and, for the direct comparison, a proton affinity of 8.29 eV (799.5 kJ/mol) was obtained for the formation of the carbonyl-protonated form (see Appendix A and Table 9).

For the *n*-butyl esters, the transfer of the first H-atom undoubtedly leads to the formation of the OH group of a preformed carboxylic group. However, a competing potential transfer of the second H-atom to the nitrogen of a pyridinic core requires large transition states. On the time scale of the mass spectrometric detection, the efficiency of such a rearrangement is expected to be very low. Furthermore, the corresponding aliphatic neutral radicals are not preformed in an intramolecular reaction mechanism.

For NABE, due to the lack of experimental data for the $C_4H_7^\bullet$ radical, additional arguments for the actual protonation site of the NAH^+ ion are derived from the subsequent fragmentation, the loss of H_2O.

$$NAH^+ \rightarrow C_6H_4NO^+ + H_2O \qquad (21)$$

Underlying the questionable NAH^+ enthalpy of formation, the thermochemical reaction (21) enthalpy raises from 1.40 to 2.31 eV.

The higher value is in contradiction to the strong intensity of the metastable fragmention of NAH^+ ions to $C_6H_4NO^+$

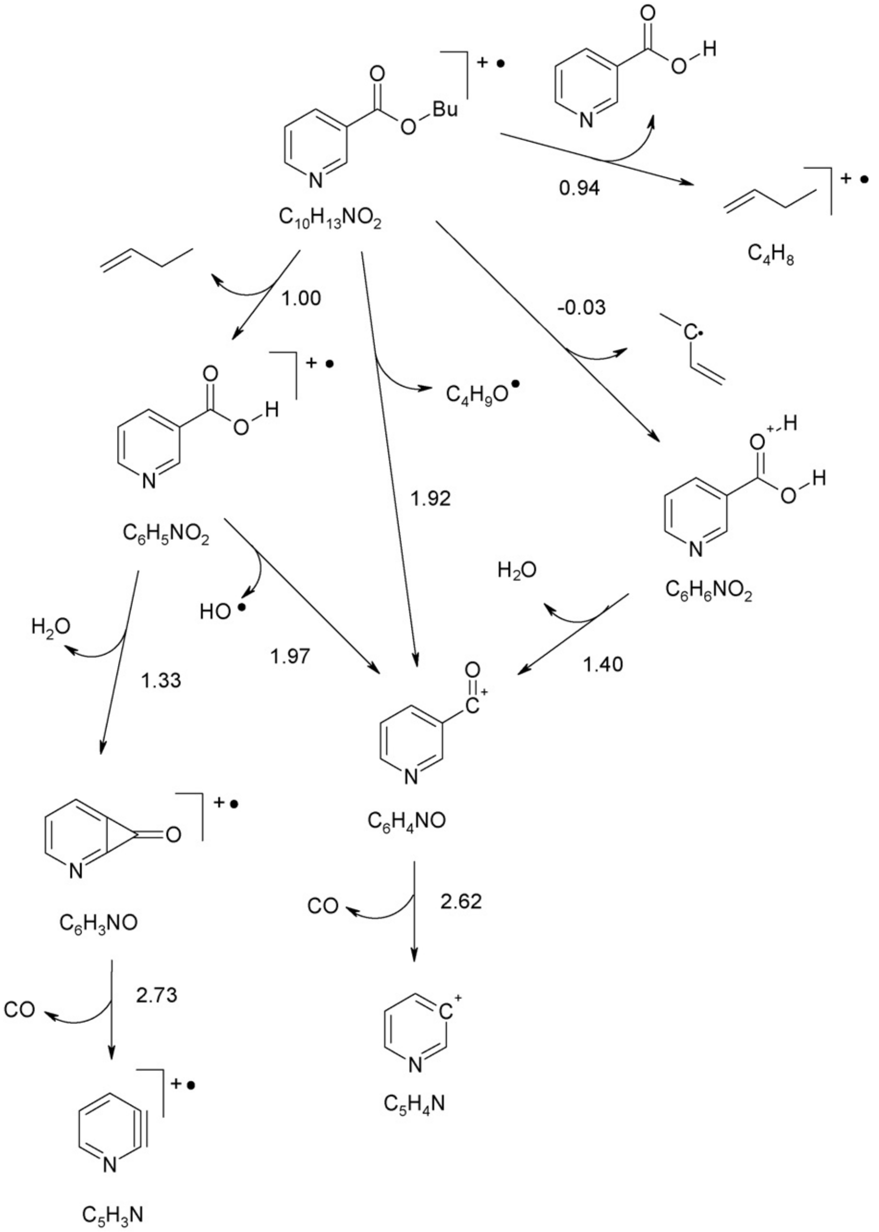

Fig. 7. Derived thermochemical reaction enthalpies (in eV) for the fragmentation of nicotinic acid *n*-butyl ester.

at *m*/*z* 106, especially in view of the comparable results for the elimination of H_2O from the protonated benzoic acid (Tables 6 and 7). In some support are results for tropic acid $C_6H_5CH(CH_2OH)COOH$, where the carboxyl group is converted into a dihydroxy form by elimination of H_2CO in a McLafferty H-transfer rearrangement. The subsequent predominant elimination of H_2O is characterized by a strong intensity of the corresponding metastable ions.

In summary, the comparison with the BABE system gives good evidence, that the mechanism of the protonation is very

Table 9
Electronic and total vibrational energies at 298 K and zero-point energies (E_{elec}, E_{vib}, ZPE) in hartree for nicotinic acid (NA) and its N- and CO-protonated forms (NA(NH^+) and NA(COH^+), respectively) according to the B3LYP DFT Gaussian 03 calculation

Species	E_{elec}	E_{vib}	ZPE	ΔE_{elec}	ΔE_{vib}	ΔH_{r}
NA	−437.000159352	0.107922	0.103707			
NA(NH^+)	−437.361233704	0.121854	0.117553	9.82534	−0.37911	9.51
NA(COH^+)	−437.314286203	0.119892	0.115133	8.54783	−0.32572	8.29

See Appendix A for the corresponding basis sets. Energy differences (ΔE) between the corresponding protonated forms and NA together with the reaction enthalpy (ΔH_{r}) for the deprotonation, as calculated according to formula (A2), are given in eV. ΔH_{r} is equivalent to the regiospecific proton affinity of NA.

similar for the two esters. Therefore, for NABE, the actual protonation site is tentatively to be the carbonyl group. Apparently, on the mass spectrometric time scale, a rearrangement to the thermochemically favoured stable products, the core-protonated acid and the methylallyl radical, is not observed. An ion/molecule complex is expected to be "smooth" enough to adopt a configuration which allows a reaction to products at the thermodynamic optimum. Therefore, this regioselectivity provides some evidence against such an ion/molecule complex as intermediate.

For the next prominent fragment ion, $C_6H_4NO^+$ ions at *m*/*z* 106, the metastable ion analysis confirms three formation channels. As discussed, intermediate $C_6H_6NO_2{}^+$ (NAH^+) ions at *m*/*z* 124 are precursors for the formation of $C_6H_4NO^+$ ions.

$$\text{NABE} \rightarrow C_6H_4NO^+ + H_2O + C_4H_7{}^{\bullet} + e^- \tag{22}$$

Using the derived formation enthalpy of this fragment ion, a reaction (22) enthalpy of $\Delta H_r = 11.34$ eV is obtained.

On the second pathway, a reaction (23) enthalpy of $\Delta H_r = 11.89$ eV is obtained.

$$\text{NABE} \rightarrow C_6H_4NO^+ + C_4H_9O^{\bullet} + e^- \tag{23}$$

This process correlates nicely with the experimental AE $(106^+) = 11.71$ eV. Reaction (22) is thermochemically favoured over reaction (23) by 0.55 eV. With respect to the given experimental error limit, some evidence is provided for the existence of an activation barrier of at least 0.6 eV for this H_2O elimination. The third process from molecular ions via intermediate formation of nicotinic acid ions and subsequent loss of an $OH^{\bullet}$ radical needs a reaction (24) enthalpy of 12.94 eV and can definitely be ruled out at energetic threshold conditions.

$$\text{NABE} \rightarrow C_6H_4NO^+ + HO^{\bullet} + C_4H_8 + e^- \tag{24}$$

As confirmed by the metastable ion decay, $C_6H_3NO^{\bullet+}$ ions at *m*/*z* 105 are dominantly formed by H_2O elimination of intermediate $C_6H_5NO_2{}^{\bullet+}$ ($NA^{\bullet+}$) ions at *m*/*z* 123.

$$\text{NABE} \rightarrow C_6H_3NO^{\bullet+} + H_2O + C_4H_8 + e^- \tag{25}$$

A reaction (25) enthalpy of 12.30 eV is calculated, which agrees very well with the experimental AE $(105^+) = 12.15$ eV.

Finally, $C_5H_4N^+$ ions at *m*/*z* 78, with an appearance energy of AE $(78^+) = 14.40$ eV, can be formed by two different processes as confirmed by the metastable ion decay. The first process is the elimination of CO from intermediate $C_6H_4NO^+$ ions.

$$\text{NABE} \rightarrow C_5H_4N^+ + CO + C_4H_9O^{\bullet} + e^- \tag{26}$$

A reaction (26) enthalpy of $\Delta H_r = 14.51$ eV is obtained.

The difference of the two appearance energies, AE (78^+) and AE (106^+), of 2.69 eV is in very good correlation with the result of 2.62 eV obtained for the pure nicotinic acid.

The second process comprises the elimination of H_2O from intermediate $NAH^{\bullet+}$ ions at *m*/*z* 124 with a reaction (27) enthalpy of $\Delta H_r = 13.96$ eV.

$$\text{NABE} \rightarrow C_5H_4N^+ + CO + H_2O + C_4H_7{}^{\bullet} + e^- \tag{27}$$

The formation via intermediate nicotinic acid according to reaction (28)

$$\text{NABE} \rightarrow C_5H_4N^+ + CO + HO^{\bullet} + C_4H_8 + e^- \tag{28}$$

with $\Delta H_r = 15.56$ eV can definitely be ruled out at energetic threshold conditions.

This leaves reaction (26) as the most probable pathway and, again, the thermochemically favoured reaction (27) comprising the elimination of H_2O from the protonated acid seems to occur with a significant activation energy.

4. Conclusions

Using ionization and appearance energies, a pathway has been presented for the determination of enthalpies of formation of the parent compounds where fragment ions are formed via a McLafferty rearrangement to well defined products with known thermochemical properties. The involved intrinsic γ-H-transfer has been found to occur without significant activation energy. This is rationalized by an initial charge-induced weakening of the corresponding C–H bond with formation of a hydrogen bridge as the transition state.

In addition, the competing double H-atom transfer from the aliphatic ester chain has been used for the determination of a proton affinity of benzoic acid and nicotinic acid. As illustrated in Fig. 3, the "driving force" for this mechanism seems to be the charge switching between the carboxyl oxygens resulting in two sequential H-transfers via an intermediate distonic ion. The absence of significant activation energies is rationalized as described for the classical McLafferty rearrangement. As expected from a regiospecific rearrangement process, the obtained proton affinities reflect the value of a protonated carbonyl group rather than, in the case of nicotinic acid, that of a protonated pyridinic nitrogen. Therefore, this method could open a gateway for the determination of regioselective proton affinities. Furthermore, on the way from a proton affinity to the determination of a (radical) cation affinity, the intermediate distonic ion in Fig. 2 thermochemically represents, at least formally, cationized benzoic acid with the specific radical cation being that of 1-butene (as example).

Acknowledgements

The author thanks Prof. A.S.K. Hashmi for reading the manuscript, Dr. S. Förster for electronic literature database searching and Dr. B. Miehlich for performing the DFT calculations.

Appendix A

The B3LYP DFT molecular orbital approach was performed with the Gaussian 03 program [32] for nicotinic acid in comparison to its N- and CO-protonated forms. A planar molecule in the trans-configuration of the carboxyl-OH with respect to the pyridinic nitrogen was selected. The geometry optimization and the frequency analysis was carried out with the 6-31 + G(d,p) basis set. Final electron energies were obtained with the optimized geometries using the 6-311 + G(2d,2p) basis set.

The proton affinity of a neutral molecule (M) was calculated as the enthalpy change at standard conditions (298 K, 1 atm) in reaction (A1) according to formula (A2).

$$\mathrm{MH}^+ \rightarrow \mathrm{M} + \mathrm{H}^+ \qquad \text{(A1)}$$

$$\mathrm{PA}(298) = \Delta E_{\mathrm{elec}} + \Delta E_{\mathrm{vib}} + \Delta E_{\mathrm{rot}} + \Delta E_{\mathrm{trans}} + \Delta(\mathrm{PV}) \qquad \text{(A2)}$$

ΔE_{elec} denotes the difference of the internal electronic energies, ΔE_{vib} the difference in the vibrational energies including their corresponding zero point energies, ΔE_{rot} the difference in the rotational energies and $\Delta E_{\mathrm{trans}}$ the difference in the translational energies. The Δ(PV) term represents the work at constant pressure. The results are summarized in Table 9. Since one species is converted into two and H^+ carries neither rotational nor vibrational energy, $\Delta E_{\mathrm{rot}} = 0$, $\Delta E_{\mathrm{trans}} = 3/2\ RT$ ($\equiv$0.03854 eV at 298 K) and $\Delta(\mathrm{PV}) = RT$ ($\equiv$0.0259 eV at 298 K) were used following the classical thermodynamic approach. In this context, some commonly applied simplifications for the evaluation of mass spectrometric appearance energy data are stated: the Δ(PV) work can be ignored due to the low pressure conditions. At energetic threshold conditions, $\Delta E_{\mathrm{trans}} \approx 0$ is assumed since no significant extra kinetic energy is transferred into the products. The initial product pair of charged and neutral species is separated in the external electric or magnetic field. Concerning the importance of the temperature correction of the products, the data in Table 9 give an impression for reaction (18). For NA, as one of the products, the difference in the vibrational energy content between 0 and 298 K is only 0.1 eV.

References

[1] H.M. Rosenstock, K. Draxl, B.W. Steiner, J.T. Heron, J. Phys. Chem. Ref. Data, Natl. Bureau Standards 6 (1977).
[2] P. Potzinger, G. von Bünau, Ber. Bunsenges. Phys. Chem. 73 (1969) 466.
[3] G. Lias, J.E. Bartmess, Gas-Phase Ion Thermochemistry, http://webbook.nist.gov/chemistry/ion.
[4] J.L. Holmes, F.P. Lossing, P.M. Mayer, J. Am. Chem. Soc. 113 (1991) 9723.
[5] J. Opitz, Int. J. Mass Spectrom. Ion Proc. 107 (1991) 503.
[6] J. Opitz, D. Bruch, K. Banert, Int. J. Mass Spectrom. Ion Proc. 115 (1992) 53.
[7] J. Opitz, D. Bruch, K. Banert, G. von Bünau, Org. Mass Spectrom. 27 (1992) 1105.
[8] J. Opitz, P. Härter, Int. J. Mass Spectrom. Ion Proc. 121 (1992) 183.
[9] J. Opitz, D. Bruch, G. von Bünau, Org. Mass Spectrom. 28 (1993) 405.
[10] J. Opitz, D. Bruch, Int. J. Mass Spectrom. Ion Proc. 124 (1993) 157.
[11] J. Opitz, D. Bruch, G. von Bünau, Int. J. Mass Spectrom. Ion Proc. 125 (1993) 215.
[12] D. Bruch, J. Opitz, G. von Bünau, Int. J. Mass Spectrom. Ion Proc. 171 (1997) 147.
[13] J. Opitz, Eur. J. Mass Spectrom. 7 (2001) 55.
[14] J. Opitz, Int. J. Mass Spectrom. 225 (2003) 115.
[15] J. Opitz, Eur. J. Mass Spectrom. 11 (2005) 371.
[16] J. Opitz, in preparation.
[17] F.M. Benoit, A.G. Harrison, Org. Mass Spectrom. 11 (1976) 1056.
[18] F.M. Benoit, A.G. Harrison, F.P. Lossing, Org. Mass Spectrom. 12 (1977) 78.
[19] S. Tajima, T. Azami, H. Shizuka, T. Tsuchiya, Org. Mass Spectrom. 14 (1979) 499.
[20] S. Meyerson, Org. Mass Spectrom. 24 (1989) 652.
[21] D.R. Lide (Ed.), Handbook of Chemistry and Physics, CRC Press, Boca Raton, Florida, USA, 1997.
[22] http://webbook.nist.gov.
[23] (a) L. Klasinc, B. Kovac, H. Gusten, Pure Appl. Chem. 55 (1983) 289;
(b) J. Meeks, A. Wahlborg, S.P. McGlynn, J. Electron Spectrosc. Rel. Phenom. 22 (1981) 43;
(c) F. Benoit, Org. Mass Spectrom. 7 (1973) 295;
(d) F. Benoit, Org. Mass Spectrom. 7 (1973) 1407;
(e) A. Foffani, S. Pignataro, B. Cantone, F. Grasso, Z. Phys. Chem. (Frankfurt) 42 (1964) 221;
(f) S. Tajima, T. Azami, T. Tsuchiya, Org. Mass Spectrom. 12 (1977) 24.
[24] D. Dougherty, E.S. Younathan, R. Voll, S. Abdulnur, S.P. McGlynn, J. Electron Spectrosc. Relat. Phenom. 13 (1978) 379.
[25] J. Bickerton, G. Pilcher, J. Chem. Thermodyn. 16 (1984) 373.
[26] T.J.D. Jörgensen, G. Bojesen, Eur. J. Mass Spectrom. 4 (1998) 39.
[27] Yu-Ran Luo (Ed.), Handbook of Bond Dissociation Energies in Organic Compounds, CRC Press, Boca Raton, Florida, USA, 2003.
[28] M.B. Stringer, D.J. Underwood, J.H. Bowie, C.E. Allison, K.F. Donchi, P.J. Derrick, Org. Mass Spectrom. 27 (1992) 270.
[29] R. Neeter, N.M.M. Nibbering, Org. Mass Spectrom. 5 (1971) 735.
[30] (a) H.-F. Grützmacher, J. Hübner, Org. Mass Spectrom. 2 (1969) 649;
(b) S.K. Pollack, W.J. Hehre, Tetrahedron Lett. 21 (1980) 2483;
(c) J.M. Riveros, S. Ingeman, N.M.M. Nibbering, J. Am. Chem. Soc. 113 (1991) 1053;
(d) P.G. Wenthold, J.A. Paulino, R.R. Squires, J. Am. Chem. Soc. 113 (1991) 7414;
(e) M.J.S. Dewar, T.P. Tien, J. Chem. Soc. Chem. Commun. (1985) 1243;
(f) X. Zhang, P. Chen, J. Am. Chem. Soc. 114 (1992) 3147.
[31] S. Bourcier, Y. Hoppilliard, Int. J. Mass Spectrom. 217 (2002) 231.
[32] M.J. Frisch, G.W. Trucks, H.B. Schlegel, G.E. Scuseria, M.A. Robb, J.R. Cheeseman, J.A. Montgomery, T. Vreven, K.N. Kudin, J.C. Burant, J.M. Millam, S.S. Iyengar, J. Tomasi, V. Barone, B. Mennucci, M. Cossi, G. Scalmani, N. Rega, G.A. Petersson, H. Nakatsuyi, M. Hada, M. Ehara, K. Toyota, R. Fukuda, J. Hasegawa, M. Ishida, T. Nakajima, Y. Honda, O. Kitao, H. Nakai, M. Klene, X. Li, J.E. Knox, H.P. Hratchian, J.B. Cross, V. Bakken, C. Adamo, J. Jaramillo, R. Gomperts, R.E. Stratmann, O. Yazyev, A.J. Austin, R. Cammi, C. Pomelli, J.W. Ochterski, P.Y. Ayala, K. Morokuma, G.A. Voth, P. Salvador, J.J. Dannenberg, V.G. Zakrzewski, S. Dapprich, A.D. Daniels, M.C. Strain, O. Farkas, D.K. Malick, A.D. Rabuck, K. Raghavachari, J.B. Foresman, J.V. Ortiz, Q. Cui, A.G. Baboul, S. Clifford, J. Cioslowsky, B.B. Stevanov, G. Liu, A. Liashenko, P. Piskorz, I. Komaromi, R.L. Martin, D.J. Fox, T. Keith, M.A. Al-Laham, C.Y. Peng, A. Nanayakkara, M. Challacombe, P.M.W. Gill, B. Johnson, W. Chen, M.W. Wong, C. Gonzalez, J.A. Pople, Gaussian 03, Rev. C.02, Gaussian, Inc., Wallingford, CT, 2004.